

# Accurate projector calibration method by using an optical coaxial camera

Shujun Huang,<sup>1</sup> Lili Xie,<sup>1</sup> Zhangying Wang,<sup>1</sup> Zonghua Zhang,<sup>1,3,\*</sup>  
Feng Gao,<sup>2</sup> and Xiangqian Jiang<sup>2</sup>

<sup>1</sup>School of Mechanical Engineering, Hebei University of Technology, Tianjin 300130, China

<sup>2</sup>Centre for Precision Technologies, University of Huddersfield, Huddersfield HD1 3DH, UK

<sup>3</sup>e-mail: zhzhzhang@hebut.edu.cn

\*Corresponding author: zhzhzhangtju@hotmail.com

Received 16 September 2014; revised 30 November 2014; accepted 18 December 2014;  
posted 22 December 2014 (Doc. ID 223112); published 26 January 2015

Digital light processing (DLP) projectors have been widely utilized to project digital structured-light patterns in 3D imaging systems. In order to obtain accurate 3D shape data, it is important to calibrate DLP projectors to obtain the internal parameters. The existing projector calibration methods have complicated procedures or low accuracy of the obtained parameters. This paper presents a novel method to accurately calibrate a DLP projector by using an optical coaxial camera. The optical coaxial geometry is realized by a plate beam splitter, so the DLP projector can be treated as a true inverse camera. A plate having discrete markers on the surface is used to calibrate the projector. The corresponding projector pixel coordinate of each marker on the plate is determined by projecting vertical and horizontal sinusoidal fringe patterns on the plate surface and calculating the absolute phase. The internal parameters of the DLP projector are obtained by the corresponding point pair between the projector pixel coordinate and the world coordinate of discrete markers. Experimental results show that the proposed method can accurately calibrate the internal parameters of a DLP projector. © 2015 Optical Society of America

*OCIS codes:* (120.0120) Instrumentation, measurement, and metrology; (120.5050) Phase measurement; (150.1488) Calibration.

<http://dx.doi.org/10.1364/AO.54.000789>

## 1. Introduction

With the maturation of digital micromirror device (DMD) technique, digital light processing (DLP) projectors based on DMD have been widely utilized in 3D shape measuring systems to project digital structured-light patterns due to their advantages of high contrast, high intensity, flexible programming, and cost efficiency [1]. 3D calibration of these systems is an important step to obtain accurate shape data [2,3]. However, the existing off-the-shelf DLP projectors are made for lecture presentations and have large lens distortion due to nonlinear factors which

cannot be compensated by the classical pinhole camera model. Therefore, it is important to calibrate the DLP projectors to obtain the internal parameters to improve the accuracy of 3D shape measuring systems.

A projector has the same physical principle and mathematical model as a camera, which can be regarded as an inverse camera. However, the projector cannot capture images like a camera. Many projector calibration methods have been studied and they can be divided into three categories. The first category is to use a calibrated camera to determine the geometric parameters of projectors [4–6]. By using a liquid-crystal display (LCD) panel as the calibration target, Song and Chung proposed to first calibrate the CCD camera and then the DLP projector [4]. Ma *et al.*

studied lens distortion of the projector by a precalibrated camera [5]. Falcao *et al.* relied on a precalibrated camera to establish the relationship between the camera and a projector [6]. Because these methods used a calibrated camera to determine the parameters of projectors, the error of the calibrated camera will accumulate to the projector and the accuracy of projector calibration is influenced by that of camera calibration. Some experiments demonstrated that the error of projector calibration is one order of magnitude larger than that of camera calibration [5].

The second category of projector calibration is to find one homography transformation between a calibration plane and the projector image plane [7–9]. Chen and Chien presented a two-stage easy-to-deploy strategy to robustly calibrate both intrinsic and extrinsic parameters of a projector [7]. Because of an iterative procedure, this method is complicated in actual application. Anwar *et al.* studied a projector calibration method by moving the projector to several locations to build up the homography between the projector and the camera [8]. Moreno and Taubin proposed a method to build up the relationship between the world coordinates and the projector pixel coordinates by using local homographies [9]. For all these methods by using homography transformation, the calibrated parameters are not accurate because homography is a linear operator and cannot model nonlinear distortion of the projector lens.

The third category of projector calibration is to create DMD images [10,11]. Zhang and Huang [10] and Li and Shi [11] presented novel projector calibration methods by generating DMD images. At different positions, after establishing the correspondence between camera pixels and projector pixels, the DLP projector can be treated as an inverse camera to create DMD images. However, the projecting axis of the DLP projector is not along the imaging axis of the CCD camera because of the crossed-optical-axes geometry of the projector and camera, so that the calibrated parameters of the projector are inaccurate.

Therefore, the existing methods either have complicated procedures by iteratively adjusting a projected pattern until it overlaps a printed pattern, or low accuracy of the obtained parameters because of dependence on the camera calibration and the crossed-optical-axes geometry of the projector and camera.

This paper presents a novel method to accurately calibrate a DLP projector by using an optical coaxial camera. A plate beam splitter is used to make the imaging axis of the CCD camera and the projecting axis of the DLP projector be coaxial, so the DLP projector can be treated as a true inverse camera and can be calibrated by using a plate having discrete markers on the surface. The corresponding projector pixel coordinate of each marker is determined by measuring its absolute phase from the projected vertical and horizontal sinusoidal fringe patterns on the

plate surface. Like camera calibration by using a checkerboard [12], the internal parameters of the DLP projector can be calibrated by using a plate having discrete markers. The following section describes the details of this calibration technique. Section 3 presents some experiments on calibrating an actual DLP projector by using the proposed method and the method based on the crossed-optical-axes geometry. Some concluding remarks and discussions are given in Section 4.

## 2. Principle

### A. Coaxial Structure of the Camera and Projector

Because a projector can be regarded as an inverse camera, both of them have the same physical principle and mathematical model. The projector cannot capture images like the camera. However, the projector can indirectly capture images by establishing a relationship between the projector and the camera, so that the projector can be calibrated like a camera. Several factors affect the calibrated results, such as symmetry of the calibration plate with respect to optical axis, the flatness of the manufactured calibration plate, the accuracy of the checker size on the checkerboard (or the separation between markers on the plate surface), the accurate extraction of the grid corner of each checker (or the center position of each marker) from the captured calibration plate images, and the numbers of the captured images at different calibration plate positions [13]. Therefore, when calibrating the camera, the calibration plate needs to be arbitrarily placed at several symmetrical orientations along the imaging axis. Otherwise, the unsymmetrically obtained images cannot give accurate internal parameters, especially the principal points. For the same reason, a calibration plate for calibrating the projector needs to be placed at several symmetrical positions along the projecting axis of the projector. If the calibration plate is placed symmetrically along the imaging optical axis of the camera for the crossed-optical-axes geometry of the projector and camera, the plate is unsymmetrical along the projecting axis and the calibrated parameters of the projector are not accurate. The calibration plate can be placed along the imaging axis of the camera and along the projecting axis of the projector, as demonstrated in Figs. 1(a) and 1(b), respectively. In both situations, the calibration plate cannot be symmetrically placed along the two axes because of the crossed-optical-axes geometry of the projector and camera.

A coaxial structure of the projector and camera can solve this problem by using a plate beam splitter, as shown in Fig. 2. The plate beam splitter makes the imaging axis of the CCD camera and the projecting axis of the DLP projector coaxial, so the DLP projector can be treated as a true inverse camera. A black plate is used to avoid the effects of environment and objects in front of the camera on the captured calibration plate image, as shown in Fig. 2. After building

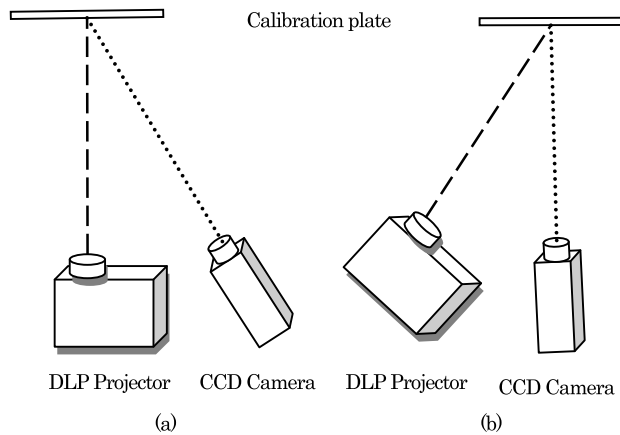


Fig. 1. Crossed-optical-axes geometry of the projector and camera. (a) Calibration plate symmetrically placed along the projecting axis of the projector and (b) calibration plate symmetrically placed along the imaging axis of the camera.

the pixel relationship between the projector and the camera, the projector can “capture” images like a camera from the same viewpoint. Therefore, the calibrated parameters of coaxial structure of the projector and camera are more accurate than that of crossed-optical-axes, especially for principal points and radial distortion of the projector lens.

#### B. Realization of the Coaxial Structure

A beam splitter with both the transmittance and the reflectance of 50% is used to realize the coaxial structure. The DLP projector projects fringe patterns onto the calibration plate. The diffuse reflected light by the plate is incident to the beam splitter from another direction. The reflected light on the calibration plate is captured by the CCD camera. The following two steps are needed to ensure the coaxial structure of the projector and the camera.

Step 1: the optical axes of the projector and the camera are in the same plane parallel to the surface of an optical tabletop.

(a) Height and angle adjustment of the projector. In principle, the optical projecting axis of the projector is at the center position of the projected images.

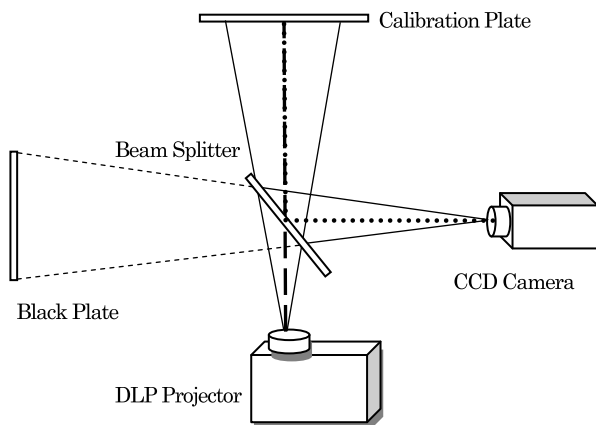


Fig. 2. Coaxial structure of the projector and camera.

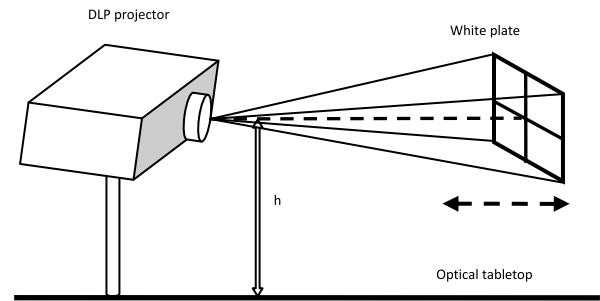


Fig. 3. Schematic diagram of the projector adjustment.

Therefore, a white cross at an image center can be generated by software and then projected onto a white plate from the projector, as illustrated in Fig. 3. When the white plate is moved back and forth on an accurate translating stage, the projected cross position on the plate surface does not move up and down, which proves that the optical projecting axis of the projector is parallel to the optical tabletop. The projected cross position on the white plate surface is marked as a reference for the following camera adjustment.

(b) Height adjustment of the camera. To adjust the imaging axis of the camera having the same height as the optical tabletop surface, the marked white plate in Step 1 is moved back and forth in front of the camera along the translating stage, as illustrated in Fig. 4. If the captured marker by the camera is always on the center position in the living images, the imaging axis of the camera is parallel to the optical tabletop surface and has the same height as the projecting axis.

Step 2: angle adjustment of the plate beam splitter. A two-dimensional manual tilt platform (from Beijing Winner Optical Instruments Co. LTD.) is used to ensure that the beam splitter is perpendicular to the optical tabletop surface, so that the diffuse reflecting light from the calibration plate can be captured by the CCD camera, as illustrated in Fig. 5. Because the projecting axis of the projector has the same height as the imaging axis of the CCD camera, the projected cross should be in the center position in the captured image if the beam splitter is perpendicular to the optical tabletop surface. At the same time, a black plate having a diffuse reflective surface is used to avoid the effects of

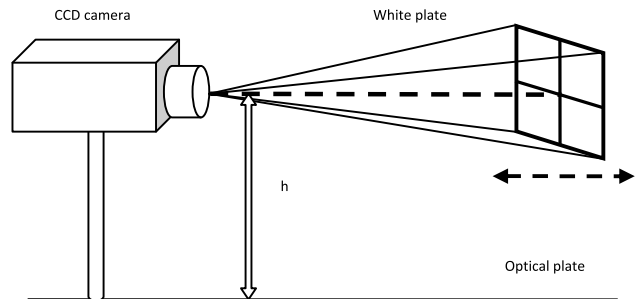


Fig. 4. Schematic diagram of the camera adjustment.

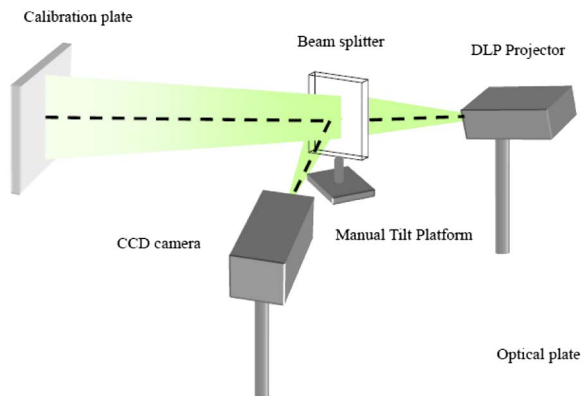


Fig. 5. Schematic diagram of the plate beam splitter adjustment.

environment and objects in front of the camera so that the captured images of the calibration plate are clear.

### C. Mathematical Model of the Projector

The mathematical model of the projector is demonstrated in Fig. 6.  $O$ - $XYZ$  and  $o$ - $xyz$  are the 3D world coordinate system and the projector coordinate system, respectively.  $O$ - $mn$  is the 2D projector pixel coordinate system.  $P_w = (X, Y, Z, 1)$  are the 3D homogeneous coordinates of a point in the world coordinate system.  $P_u = (m, n, 1)$  are the corresponding 2D homogeneous coordinates of the point in the projector pixel coordinate system. Like a camera model [10], the projector model is represented as

$$s[m \ n \ 1]^T = A[R \ T][X \ Y \ Z \ 1]^T, \quad (1)$$

where  $R$  is a matrix representing the three rotating angles,  $T = [T_x \ T_y \ T_z]$  is a vector representing the three translating distances,  $s$  is an arbitrary scaling

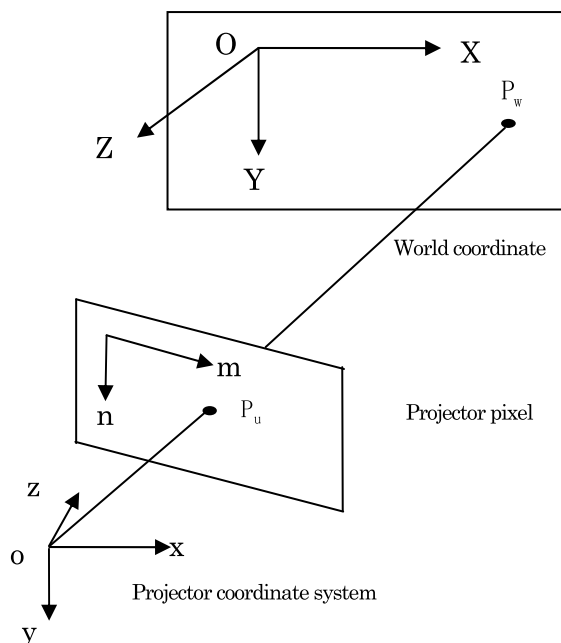


Fig. 6. Mathematical model of the projector.

factor, and  $[]^T$  denotes the transpose. Three rotating angles and three translating distances are called as external parameters of the projector.  $A$  is a matrix of partial intrinsic parameters of the projector, which can be represented as

$$A = \begin{bmatrix} f_m & 1 & m_0 \\ 0 & f_n & n_0 \\ 0 & 0 & 1 \end{bmatrix}, \quad (2)$$

where  $[m_0 \ n_0]$  are the pixel coordinates of the principal point, and  $[f_m \ f_n]$  are the focal lengths along  $m$ - and  $n$ -axes directions. To calibrate the projector model, we use a planar target assumed to lie in the plane  $Z = 0$  [13]. Thus, the  $3 \times 4$  projection matrix  $[R \ T]$  reduces to a  $3 \times 3$  homography. In practice, due to distortion of the projector lens, point  $P_w$  in the world coordinate system does not directly correspond to point  $P_u$  of the projector pixel coordinate system, but at a distorted position of point  $P_d$ . To compensate for the lens distortion, the projection model is augmented with two radial distortion terms  $k_1$  and  $k_2$ , and two tangential distortion terms  $p_1$  and  $p_2$ . The coordinates  $P_d$  can then be corrected using the following relation:

$$P_d = P_u + \delta(P_d, P_u), \quad (3)$$

where

$$\begin{aligned} \delta(P_d, P_u) &= \begin{bmatrix} m_u(k_1 r_u^2 + k_2 r_u^4) + 2p_1 m_u n_u + p_2(r_u^2 + 2m_u^2) \\ n_u(k_1 r_u^2 + k_2 r_u^4) + 2p_2 m_u n_u + p_1(r_u^2 + 2n_u^2) \end{bmatrix} \\ r_u^2 &= m_u^2 + n_u^2, \end{aligned}$$

and  $[k_1 \ k_2 \ p_1 \ p_2]$  are distortion coefficients of the projector lens. The four coefficients along with principal point  $[m_0 \ n_0]$  and focal lengths  $[f_m \ f_n]$  are internal parameters of the projector lens. Projector calibration means to obtain the eight internal parameters  $[m_0 \ n_0 \ f_m \ f_n \ k_1 \ k_2 \ p_1 \ p_2]$  and six external parameters  $[R, T]$ . In this paper, only the internal parameters are calibrated.

According to the proposed model of Eq. (1), it is possible to calibrate a projector by using a plate having discrete markers on the surface provided the corresponding projector pixel coordinate of each marker can be accurately determined in the projector pixel coordinate system. A white plate with a scattered surface was designed and manufactured for projector calibration [3]. There are  $9 \times 12$  discrete black hollow ring markers on the surface. The separation of neighboring markers along the vertical and horizontal direction has the same value of 15 mm with an accuracy of 1  $\mu$ m.

In order to build up the correspondence of discrete markers between the world coordinate system and the projector pixel coordinate system at each plate orientation, vertical and horizontal sinusoidal fringe



patterns are generated with a computer and projected onto the plate surface through the DLP projector. At each fringe direction, twelve sinusoidal fringe patterns (including three-fringe pattern sets with the optimum fringe numbers and each set having four phase-shifted fringes) are used to calculate the absolute phase of the center position of each marker [14] and one texture image under white illumination to determine the center position of each marker. The main procedure includes the following several steps to establish the pixel relationship between the projector and the camera, as illustrated in Fig. 7.

A set of horizontal and vertical sinusoidal fringe patterns are projected onto the calibration plate surface at each plate orientation. At each fringe direction, the fringe numbers are 56, 63, and 64. The coaxial camera captures the fringe pattern images and the texture map illuminated under white light. Assuming four vertical captured fringe patterns are  $I_1, I_2, I_3, I_4$  and they have  $\pi/2$  shift in between, a wrapped phase map is calculated by using a four-step phase-shifting algorithm

$$\theta = \tan^{-1}[(I_4 - I_2)/(I_1 - I_3)]. \quad (4)$$

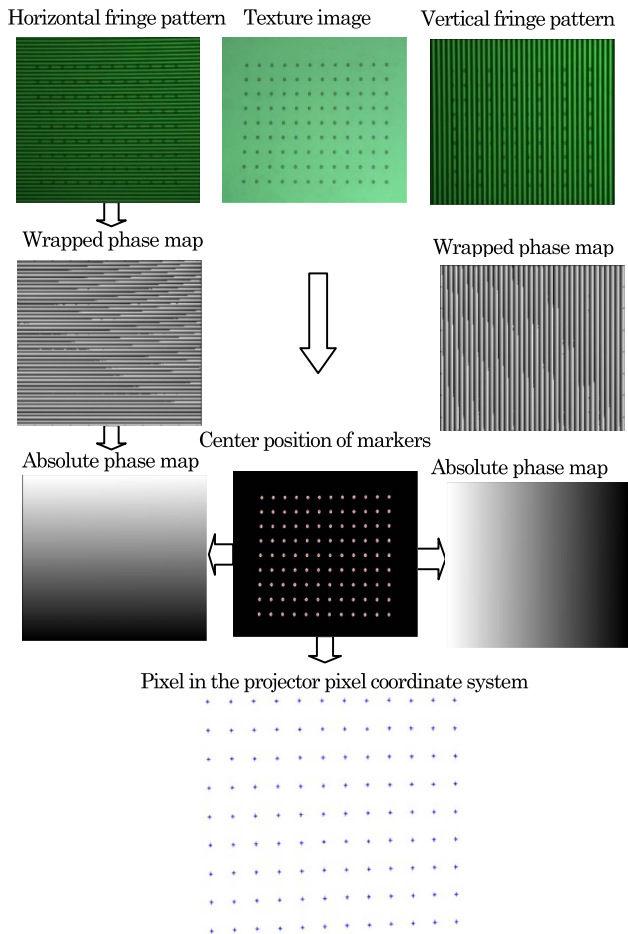


Fig. 7. Flow chart of establishing the pixel relationship between the projector and the camera.

After applying Eq. (4) to the three-fringe pattern sets, three wrapped phase maps are obtained. Due to the inverse trigonometric function in Eq. (4), the obtained modulo  $2\pi$  phase information needs to be unwrapped. In order to obtain the absolute phase information at the center of each marker, the optimum multiple-fringe numbers selection method is used to calculate the absolute fringe order pixel by pixel [14]. With three-fringe sets having fringe numbers of 56, 63, and 64, the method is referred to as the optimum three-fringe numbers selection method. This method resolves fringe order ambiguity as the beat obtained between 64 and 63 is a single fringe over the full field of view and the reliability of the obtained fringe order is maximized as fringe order calculation is performed through a geometric series of beat fringes with 1, 8, and 64 fringes. The obtained absolute phase data is unwrapped pixel by pixel. For horizontal fringe patterns, the corresponding wrapped and absolute phase maps are calculated by the same procedure.

After extracting the inner and outer edges of each hollow ring from the captured texture image, sub-pixel coordinates of the center position of each marker on the calibration plate are accurately located by an ellipse fitting algorithm [15]. The absolute phase of each marker along the vertical and horizontal direction is directly extracted from the two obtained absolute phase maps, denoted as  $[\varphi_m \varphi_n]$ . The corresponding point  $(m, n)$  in the projector pixel coordinate system is calculated by the following equations:

$$m = M\varphi_m/(2\pi F), \quad (5a)$$

$$n = N\varphi_n/(2\pi F), \quad (5b)$$

where  $M$  and  $N$  are the vertical and horizontal resolution of the DLP projector.  $F$  is the projected fringe numbers for phase calculation. Using Eqs. 5(a) and 5(b), the corresponding projector pixel coordinate of the center of all markers can be determined for all plate orientations. Similar to camera calibration using a checkerboard [12], the DLP projector can be calibrated to determine the internal parameters by using the obtained projector pixel coordinate on the white plate and their corresponding world coordinate.

### 3. Experiments and Results

The optical coaxial experimental system comprises a portable DLP video projector, a 3-CCD color camera with IEEE 1394 port, a beam splitter, and a personal computer, as illustrated in Fig. 8. The projector is from BenQ (Model CP270) with one-chip digital DMD and a resolution of up to 1024 pixels  $\times$  768 pixels (XGA). The 3-CCD camera from Hitachi (Model HVF22F) has a resolution of 1360 pixels  $\times$  1024 pixels. The beam splitter has the transmittance and the reflectance of 50%. A white cross in center of

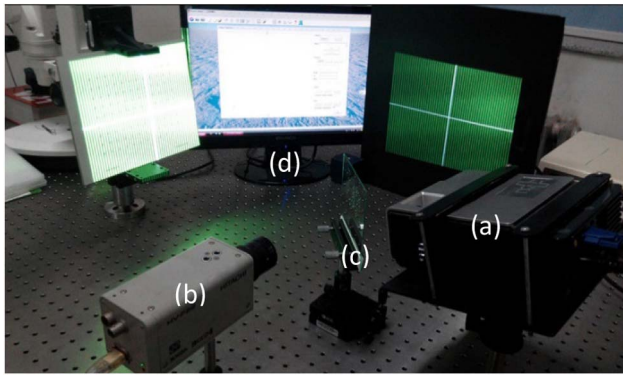


Fig. 8. Optical coaxial experimental system. (a) A DLP projector, (b) a color 3-CCD camera, (c) a beam splitter, and (d) a personal computer.

the generated image is projected onto the middle of the field from the projector to locate the object in the calibrated field of view.

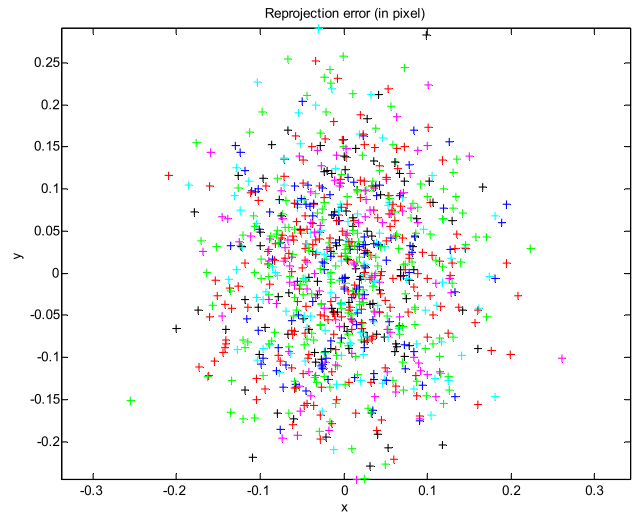
The calibration plate was randomly placed at several different orientations in front of the projector. At each orientation, vertical and horizontal sinusoidal fringe patterns were projected onto the plate surface. The CCD camera captured the fringe pattern images and a texture image under white illumination. They were saved to a computer for post-processing. After the absolute phase and the center position of all markers was determined by the proposed method, the corresponding point of each marker in the projector pixel coordinate system can be obtained by using Eq. (5). Using all the obtained corresponding point pairs at all the plate orientations, the internal parameters of the projector were calibrated, as listed in the middle row of Table 1. In comparison, the internal parameters of the same projector were calibrated by using the crossed-optical-axes geometry, as listed in the bottom row of Table 1. It clearly shows that the principal point in row direction calibrated by the coaxial geometry is much closer to the center position than that by the crossed-optical-axes geometry. In column direction, both methods give the principal point deviating from the center significantly, because the projector is designed to project images along an off-axis direction.

In order to evaluate the calibrated internal parameters, the reprojection error distributions of the projector are calculated for all the plate orientations, as show in Fig. 9. The average reprojection errors are 0.07646 and 0.08779 for the optical coaxial geometry and the crossed-optical-axes geometry, respectively. In order to further evaluate the proposed method,

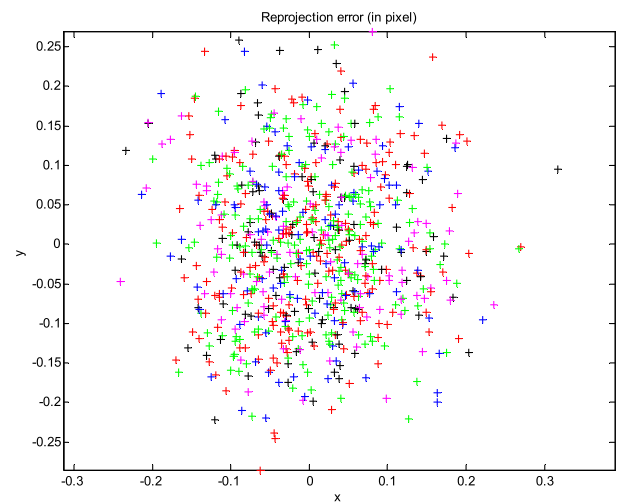
Table 1. Internal Parameters of the Calibrated Projector<sup>a</sup>

$m_0$	$n_0$	$f_m$	$f_n$	$k_1$	$k_2$	$p_1$	$p_2$
505.7	219.4	2175.9	2160.5	0.1114	0.7833	0.0090	0.0007
483.2	223.9	2209.6	2205.8	0.1141	0.9059	0.0107	0.0035

<sup>a</sup>Unit: pixel for  $m_0$ ,  $n_0$ ,  $f_m$ , and  $f_n$ .



(a) error = [ 0.07646 0.09627 ]



(b) error= [0.08779 0.09849]

Fig. 9. Reprojection error: (a) reprojection error of coaxial structure and (b) reprojection error of crossed-optical-axes structure.

the same projector was calibrated by the existing projector calibration methods in [6,9,10]. Table 2 shows the average reprojection error by using different projector calibration methods.

The average reprojection error of the proposed method is better than that of the existing projector calibration methods. The experimental results testify that the proposed method based on optical coaxes geometry accurately calibrates the principal points and the radial distortion coefficients of a DLP projector lens. Since the white plate can be placed randomly in the projecting field of volume, the proposed projector calibration method is simple and flexible. The CCD camera is just used to capture

Table 2. Average Reprojection Error by Using Different Methods<sup>a</sup>

Method	G. Falcao	D. Moreno	S. Zhang	Our Method
Average error	0.8671	0.1447	0.2176	0.0764

<sup>a</sup>Unit: pixel.

fringe patterns and texture images for calculating the absolute phase of each marker and determining marker center, respectively, so the proposed projector calibration method is independent of the camera.

#### 4. Conclusions

In conclusion, a novel projector calibration method has been proposed by using an optical coaxial camera to capture the calibration images of a white plate with discrete markers on the surface. A plate beam splitter has been used to make imaging axis of a CCD camera and projecting axis of a DLP projector coaxial, so the DLP projector can be treated as a true inverse camera. Vertical and horizontal absolute phase has been used to establish the point pair correspondence of the markers between the world coordinate system and the projector pixel coordinate system. The experimental results demonstrate the accuracy and flexibility of the proposed projector calibration method. Because the proposed method needs neither a calibrated camera nor a complicated procedure, it can give high accurate geometric parameters of the projector by using an optical coaxial camera in a simple and flexible way. The other advantage is the optical coaxes geometry gives a true inverse camera, so the calibrated parameters are more accurate than that of crossed-optical-axes geometry, especially the principal points and the radial distortion coefficients of the projector lens.

The uncertainty of the proposed projector calibration method depends on the calibration plate and the obtained absolute phase of each marker. On one hand, the flatness of the manufactured calibration plate and the accuracy of the extracted center position of each marker on the calibration plate have effects on the results of projector calibration. On the other hand, the proposed method depends on the projected fringe numbers, the sinusoidal shape of the captured fringe pattern, and the image resolution of the used CCD camera.

The authors would like to thank the National Natural Science Foundation of China (under grants 61171048 and 61311130138), the Program for New Century Excellent Talents in University (under grant NECT-11-0932), the Specialized Research Fund for the Doctoral Program of Higher Education ("SRFDP") (under grant 20111317120002), and the

Research Project for High-Level Talents in Hebei University (under grant GCC2014049). This project is also funded by the Royal Society's International Exchanges Scheme 2012 (under grant IE121613) and the EPSRC Centre for Innovative Manufacturing in Advanced Metrology.

#### References

1. Z. H. Zhang, "Review of single-shot 3D shape measurement by phase calculation-based fringe projection techniques," *Opt. Lasers Eng.* **50**, 1097–1106 (2012).
2. Z. H. Zhang, H. Y. Ma, T. Guo, S. X. Zhang, and J. P. Chen, "Simple, flexible calibration of phase calculation-based three-dimensional imaging system," *Opt. Lett.* **36**, 1257–1259 (2011).
3. Z. H. Zhang, S. J. Huang, S. S. Meng, F. Gao, and X. Q. Jiang, "A simple, flexible and automatic 3D calibration method for a phase calculation-based fringe projection imaging system," *Opt. Express* **21**, 12218–12227 (2013).
4. Z. Song and R. Chung, "Use of LCD panel for calibrating structured-light-based range sensing system," *IEEE Trans. Instrum. Meas.* **57**, 2623–2630 (2008).
5. S. D. Ma, R. H. Zhu, C. G. Quan, L. Chen, C. J. Tay, and B. Li, "Flexible structured-light-based three-dimensional profile reconstruction method considering lens projection-imaging distortion," *Appl. Opt.* **51**, 2419–2428 (2012).
6. G. Falcao, N. Hurtos, J. Massich, and D. Fofi, "Projector-camera calibration toolbox," Technical Report, 2009. Available at <http://code.google.com/p/procamcalib>.
7. C. Y. Chen and H. J. Chien, "An incremental target-adapted strategy for active geometric calibration of projector-camera systems," *Sensors* **13**, 2664–2681 (2013).
8. H. Anwar, I. Din, and K. Park, "Projector calibration for 3D scanning using virtual target images," *Int. J. Precis. Eng. Man.* **13**, 125–131 (2012).
9. D. Moreno and G. Taubin, "Simple, accurate, and robust projector-camera calibration," in *3D Imaging, Modeling, Processing, Visualization and Transmission (3DIMPVT)*, Zurich, Switzerland, October 2012.
10. S. Zhang and P. S. Huang, "Novel method for structured light system calibration," *Opt. Eng.* **45**, 083601 (2006).
11. Z. W. Li and Y. S. Shi, "Projector calibration algorithm for the structured light measurement technique," *Acta Opt. Sinica* **11**, 3061–3065 (2009).
12. Z. Y. Zhang, "A flexible new technique for camera calibration," *IEEE Trans. Pattern Anal.* **22**, 1330–1334 (2000).
13. Z. Y. Zhang, "A flexible new technique for camera calibration," Technical Report MSR-TR-98-71 (Microsoft Research, 1998). Available at <http://research.microsoft.com/~zhang/Calib/>.
14. Z. H. Zhang, C. E. Towers, and D. P. Towers, "Time efficient colour fringe projection system for 3-D shape and colour using optimum 3-frequency interferometry," *Opt. Express* **14**, 6444–6455 (2006).
15. A. Fitzgibbon, M. Pilu, and R. B. Fisher, "Direct least square fitting of ellipses," *IEEE Trans. Pattern Anal.* **21**, 476–480 (1999).